JOURNAL OF MATERIALS SCIENCE: MATERIALS IN MEDICINE 6 (1995) 335–339

Thermal wave non-destructive thickness measurements of hydroxyapatite coatings applied to prosthetic hip stems

A. C. BENTO
Universidade Estadual de Maringá, Departamento de Fisica, Av. Colombo 3690, Maringá-PR 87020-900, Brazil

S. R. BROWN, D. P. ALMOND, I. G. TURNER
School of Materials Science, University of Bath, Claverton Down, Bath, BA2 7AY, UK

Thermal wave interferometry is a non-destructive inspection technique that has been used successfully for the assessment of coating thickness. The purpose of this paper is to present an evaluation of the suitability of the technique for the measurement and characterization of hydroxyapatite coatings on commercially available prosthetic hip stems. The results indicate a good correlation between the coating thickness values obtained using the interferometry technique and measurements made using optical microscopy of sectioned stems. In addition the results confirm that thermal wave interferometry can be used to accurately assess the changes in coating thickness on samples with a complex geometry.

1. Introduction

Osteoarthritis is a painful and crippling disability suffered by people worldwide. Each year in excess of 400 000 patients undergo hip surgery. For elderly patients, the success rate of a total hip replacement is high, 90% over a ten-year period. For those in the 16–24 year age group, who are generally more active, it can be expected that a revision operation will have to be performed approximately 3 years after initial surgery [1]. One approach to improving the life span of an artificial hip is the use of cementless fixation, which ensures the close contact of the bone to the implant surface. It is based upon bone being able to form around the implant to maintain a bond. As a consequence there is much interest in the development of bioactive coatings such as hydroxyapatite (HA) which promote bony ingrowth at the bone : implant interface [2]. HA-coated implants combine the superior mechanical performance of a metal component with the excellent biological responses of hydroxyapatite. Bioactive hydroxyapatite coatings are applied to implants using the plasma spraying technique. Such coatings, with their macroporous surfaces, can significantly improve bone ingrowth [3–7].

Plasma spraying is a type of thermal spraying process, in which the coating powder is heated near or above its melting temperature in a plasma gas stream and then accelerated towards the substrate in the gas stream. On impact a particle is cooled rapidly due to the large surface area and the temperature gradient between the particle and the substrate [8]. Plasma spraying is a line-of-sight overlay process for which the deposition of uniform coatings on complex geometry components is difficult. Monitoring the coating thickness on a typical production run is usually done by positioning test coupons close to the component and examining these using microscopy, this is a labour-intensive operation and may not always produce an accurate indication of the coating thickness on the actual component. Thermal wave interferometry is a non-destructive inspection technique which has been shown to be particularly suited to the assessment of coating thickness. It has the attractions of being rapid and non-contacting and of providing detailed profilometric information about coatings on complex components.

The purpose of this paper is to present an evaluation of the suitability of thermal wave interferometry for the measurement and characterization of HA coatings on medical implants. The work has necessitated the determination of the thermal wave response of HA coatings using a number of test pieces coated with known thickness of HA. Following the thermal wave examinations, each implant was sectioned to compare coating thicknesses obtained by optical microscopy with those indicated by thermal wave interferometry.

1.1. Thermal wave interferometry

Thermal wave techniques arose from investigations of the photoacoustic effect. They have been in use for materials characterization since Rosencwaig and Gersho [9] developed the basic theory for the photoacoustic effect in condensed matter. The techniques are all based on the generation of thermal waves by heating a sample using modulated light. The thermal waves produced may subsequently be detected by

0957–4530

a variety of means such as: microphones in a traditional photoacoustic cell; pyroelectric or piezoelectric transducers; the mirage effect in the heated medium above the sample surface or simply by an infrared sensor which provides a direct indication of the modulated heating produced at the surface [10].

The basic principle of thermal wave interferometry is that when thermal waves are generated at a coating surface, they propagate to the interface with the substrate where they are partially reflected and return to produce thermal interferences effects at the surface. The interference between the reflected and the incoming thermal waves leads to variations in the surface temperature which are related to the subsurface layered structure. Bennett and Patty [11] first presented a full theory of thermal wave interferometry (TWI) and drew attention to its potential for assessing coating thickness and thermal properties. Since then this technique has been successfully developed specifically for the non-contactive and non-destructive inspection of plasma-sprayed coatings. It has been shown to be applicable to a wide range of coating types and to provide evidence of coating defects as well as determining coating thickness [12, 13].

1.2. Theory

The thermal waves generated within a thin coating are dependent on the thermal properties of the coating material and on thermal wave interference in the coating layer.

Assuming a one-dimensional heat transfer model and uniform periodic heating, the temperature in the medium, obtained from the Fourier equation, has heavily damped wave-like characteristics. For a homogeneous semi-infinite uncoated solid, the temperature at a depth x beneath the sample is

$$T(x,t) = T_0 e^{-x/\mu} e^{-i(\omega t - x/\mu)}$$

in which $\mu = (2\alpha/\omega)^{1/2}$ is the thermal diffusion length also known as *thermal skin depth* in analogy to the skin depth of an electromagnetic wave in an electrically conductive medium. This parameter is controlled by the angular frequency of heating ω and the thermal diffusivity $\alpha = K/\rho C$ which is the ratio of thermal conductivity K and volumetric heat capacity ρC.

The changes in amplitude and phase caused by thermal wave interference in an opaque coating of thickness L have been shown to be given by [11]

$$\Theta = \frac{I_0}{2k\sigma} \frac{[1 + R\exp(-2\sigma L)]}{[1 - R\exp(-2\sigma L)]}$$

in which $\sigma = (1 + i)/\mu$ is the complex thermal wave number and I_0 is the intensity of the light absorbed at the surface. The reflection coefficient $R = (1 - b)/(1 + b)$ gives the magnitude of thermal wave reflection at an interface where the parameter $b = ((\rho CK)_s/(\rho CK)_c)^{1/2}$ is the ratio of substrate and coating effusivities. Although changes in both amplitude and phase are produced by thermal wave interference in a coating, measurements of phase are the more reliable because they are not affected by spurious effects (sample surface emissivity variations, heat source intensity fluctuations, etc). that alter thermal wave amplitude. Fig. 1 shows the characteristics of the normalized phase as a function of thermal thickness L/μ for several values of reflection coefficients R. It is clear that the intrinsic damping of the thermal wave ensures that interference effects are only significant where coating thicknesses are less than about 1.5μ. In this range there is a systematic dependence of phase on coating thickness. Consequently, provided the parameter μ is adjusted to be close to L by choosing an appropriate modulation frequency, thermal wave interference can be used as a means of assessing coating thickness.

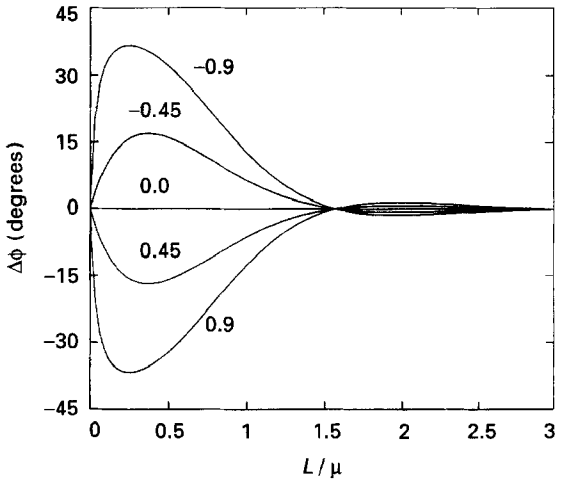

Figure 1 Normalized phase as a function of thermal thickness for a set of reflectivity coefficients R.

2. Materials and methods

2.1. Materials

Three Ti/6Al/4V alloy, BS3531, test pieces 35 × 27 × 2 mm were air plasma spray coated with HA to different thicknesses to act as standards for calibrating the thermal wave interferometry apparatus. Following this exercise, the TWI technique was applied to a commercially available HA-coated prosthetic hip stem. This particular design of stem was chosen due to its complex geometry, an outline of which is shown in Fig. 2.

2.2. Methods

2.2.1. Thermal wave experimental testing system

The thermal wave testing system is shown schematically in Fig. 3. Measurements were made by using a 5 W argon ion laser (Coherent Innova 90-5) which was adjusted to an optical power of 1.5 W. The laser was modulated by a mechanical light chopper (EG&G Brookdeal 9479) at frequencies in the range 1 to 10 Hz.

The infrared emissions from the heated spot on the sample were monitored by a pyroelectric lithium tantalate infrared detector (Philips 300 series) in which

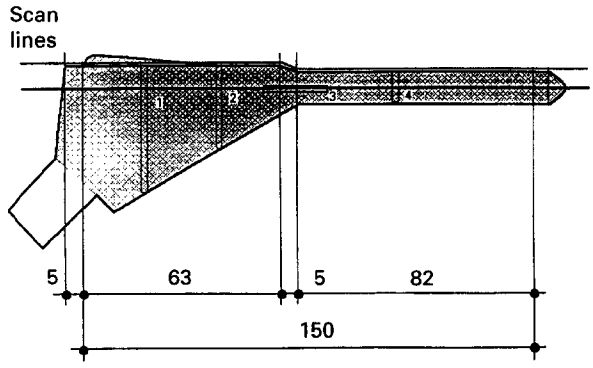

Figure 2 Commercial titanium prosthetic hip stem coated with hydroxyapatite showing the position of laser scan lines and sectioned areas, 1, 2, 3 and 4. Dimensions indicated are in millimetres.

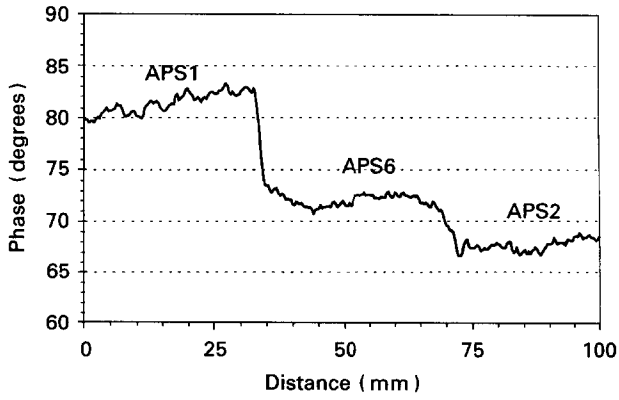

Figure 4 Thermal wave phase trace obtained from three hydroxyapatite plasma-sprayed calibration samples, coating thicknesses 95 ± 15 μm (APS1), 115 ± 10 μm (APS6) and 210 ± 20 μm (APS2). Scan frequency 4 Hz.

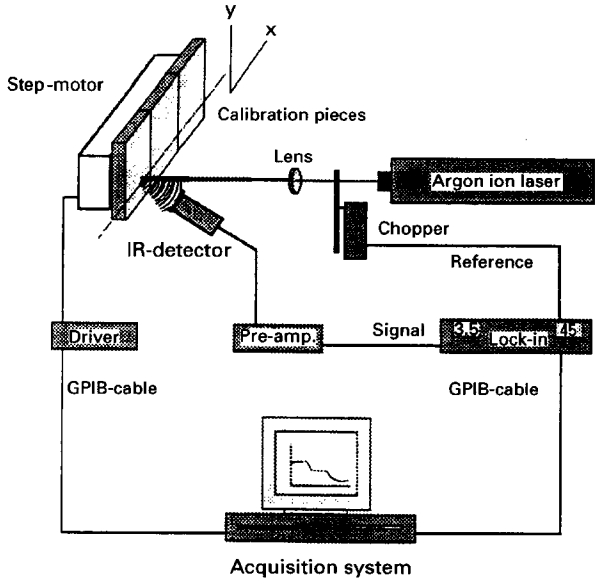

Figure 3 Thermal wave inspection system.

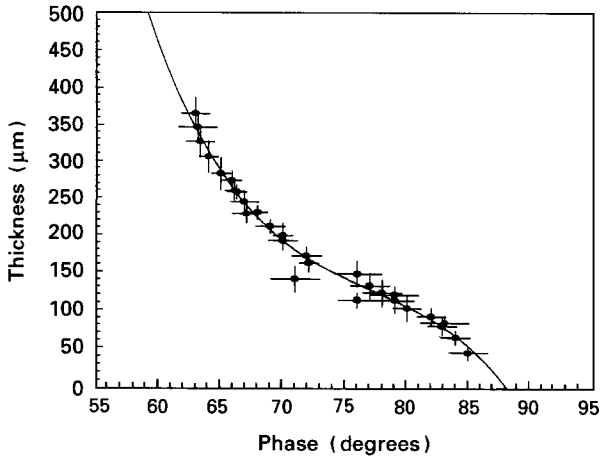

Figure 5 Hydroxyapatite calibration thickness as a function of measured thermal wave phases. Scan frequency 4 Hz.

a germanium anti-reflective coated window was used to reject scattered laser light while passing the required thermal radiation.

The signal from the detector was then processed by a lock-in analyser (EG & G PAR 5210) which monitors both the amplitude and phase of the input signal with respect to the reference signal provided by the light chopper.

The sample scanning was controlled by a step motor drive (Ealing System Five) which was adjusted to take four data points per millimetre (250 μm/step). All data acquisitions and sample scanning were controlled by a microcomputer system (Amstrad PC1512DD) interfaced with an IBM-GPIB board controller.

Calibration curve for thermal wave thickness measurement. Three coated test pieces were used to calibrate the system to provide the actual relationship between thermal wave measurements of phase and the thicknesses of the coatings. This calibration procedure was essential because the thermal properties of the plasma-sprayed coating material were unknown. The test pieces were coated with 95 ± 15 μm (APS1), 155 ± 10 μm (APS6) and 210 ± 20 μm (APS2) thicknesses of hydroxyapatite. These coating thickness measurements were obtained by the metallographic and image analysis procedure described later. The three test pieces were put side by side and scanned along 100 mm using ten different modulation frequencies in the range 1 to 10 Hz.

Fig. 4 shows a 4 Hz trace of the thermal wave phase against scanned distance. In this figure there are three different steps caused by thermal wave interference in the three coating thicknesses. These steps are not as flat as might be expected. This indicates the coating thickness to be varying along each test piece in a manner that is characteristic of the plasma spraying process.

Fig. 5 shows the phase-thickness conversion curve which was obtained from the data obtained at the ten different frequencies, normalized to 4 Hz. When only a small number of known coating thicknesses are available for calibration, measurements made at different frequencies can be combined by a simple normalization procedure to improve the accuracy of the conversion curve. As the phase is a function of L/μ rather than L alone, phase data obtained at different

frequencies can be combined by plotting it as a function of $L\sqrt{\omega}$. Alternatively this relationship may be used to normalize results to those obtained at a chosen reference frequency, such as the 4 Hz chosen here. The continuous line in this figure represents the best fitting curve from the following converting expression

$$L(\phi) = (a(\phi - b)^3 + \exp(-c\phi^2))10^3$$

where $L(\phi)$ is the coating thickness in μm, ϕ is the thermal wave experimental phase in degrees, and a, b, c are fitted parameters ($a = -3.907 \times 10^{-5}$, $b = 76.19$ and $c = 3.443 \times 10^{-4}$).

The error bars in Fig. 5 represent the standard deviation of the normalized data obtained from the three calibration samples. The horizontal error bars are the phase errors and are ranged 0.5–2.5° while the vertical bars are thickness errors from 10 to 30 μm. If they are computed in the fitted equation a net conversion error of about 10 μm results.

2.2.2. Microscopic examination of hydroxyapatite coatings

Sample preparation. Transverse sections were taken through the calibration test pieces to enable accurate measurements of the different coating thicknesses to be made using optical techniques. The prosthetic stem was sectioned transversely in three places and in addition one longitudinal section was taken through the stem where the geometry changed (Fig. 2). To prepare a cross-section of the coating it was impregnated with an epoxy resin by vacuum extracting any air trapped in the coating and then pressurizing the resin into the pores and cracks of the coating. The pressure was maintained while the resin was curing. This procedure was followed to prevent the coating from cracking and flaking when cut into suitably sized pieces for microscopic analysis. The samples were cut with a diamond saw and mounted in resin for polishing.

The samples were polished using a Buehler Motopol 12 automatic polishing and grinding machine following the sequence of grinding and polishing steps illustrated in Table I.

Image analysis. A PC-based image analyser linked in real time by a video camera to an optical microscope using normal reflective light was used to view the cross-section of the coatings. The image analysis software employed was Data Cell Optimas image processing software in Windows. The coating thickness was measured for all the plasma-sprayed hydroxyapatite coatings, by taking, on average, 150 measurements at regular intervals through the cross-section of the coating using a semi-automated process.

3. Results and discussion

The commercially available HA coated titanium hip prosthesis examined in this study is illustrated in Fig. 2. It can be seen that the design incorporates a number of significant geometry changes along the coated region. This sample was scanned for 150 mm along the lateral and anterior aspects of the stem using a frequency of 4 Hz. The variation in coating thickness measurements obtained by thermal wave interferometry is shown in Fig. 6. The bold line is the mean thickness measured and the upper and lower lines are its variations. This thickness variation is inherent to the calibration, Fig. 4, and could only be reduced if the coating thickness uniformity of the calibration test pieces could be improved. The results indicate the wide variation in the coating thickness along the length of the stem with a measurement of approximately 200 μm proximally compared to 100 μm in the distal portion.

In order to compare the thermal wave results with those obtained using the more conventional technique of optical microscopy, four sections were taken from along the length of the hip stem as illustrated in Fig. 2. Sections 1, 2, and 4 were taken perpendicular to the laser scanning line while section 3 was intentionally chosen to be parallel to the scanning line due to the geometry change found in that region. The sections were polished prior to examination using optical microscopy; thickness measurements of the coatings were then made using the image analysis system. The resulting average thicknesses and the standard deviation for sections 1, 2, and 4 are represented by the single points in Fig. 6. Section 3, parallel to the scanning line, is represented in Fig. 6 by three points. The measurements recorded indicate that the thickness almost doubles in the centre of this section which corresponds directly to the position of the change in stem geometry 60–80 mm along the scanned surface.

TABLE I Polishing procedure for plasma sprayed hydroxyapatite coatings

Step	Surface/abrasive and lubricant type	Wheel speed (rpm)	Duration (min)	Force per sample and sample rotation direction
1	Paper SiC P180 grit; water	150	3	5 lbf complimentary
2	Metlap Surface 4; 9 μm diamond oil base	25	4	5 lbf contra
3	Texmet surface 1; 1 μm diamond oil base	240	4	5 lbf complimentary
4[a]	Texmet surface 1; 0.06 μm colloidal silica	100	8	10 lbf complimentary
5	Texmet surface 1; 0.06 μm colloidal silica	100	3	2.5 lbf complimentary

[a] Check samples after 8 min, repeat until no further improvement can be seen
Complimentary: platen and specimens rotating in the same direction
Contra: platen and specimens rotating in opposite directions
Wheel speeds are for a 12 inch diameter wheel

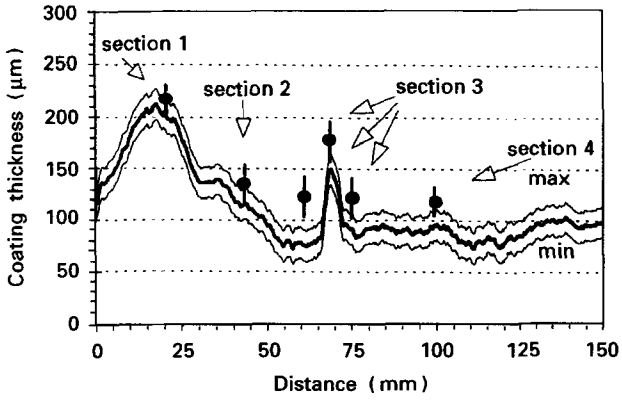

Figure 6 Coating thickness trace obtained by TWI on traversing 150 mm along the anterior of the prosthetic stem at a frequency of 4 Hz. Metallographic measurements are shown as solid points (see text).

TABLE II Coating thickness measurements of hydroxyapatite coated hip prostheses

Section	Optical microscopy (μm)	Thermal wave interferometry (μm)	
1	218 ± 14	A 205 ± 20	L 95 ± 15
2	135 ± 17	A 115 ± 10	L 145 ± 10
3	125 ± 18	A 80 ± 15	L 135 ± 10
	182 ± 18	A 150 ± 10	L 140 ± 10
	125 ± 18	A 90 ± 15	L 105 ± 15
4	112 ± 16	A 95 ± 15	L 95 ± 15

L = lateral; A = anterior

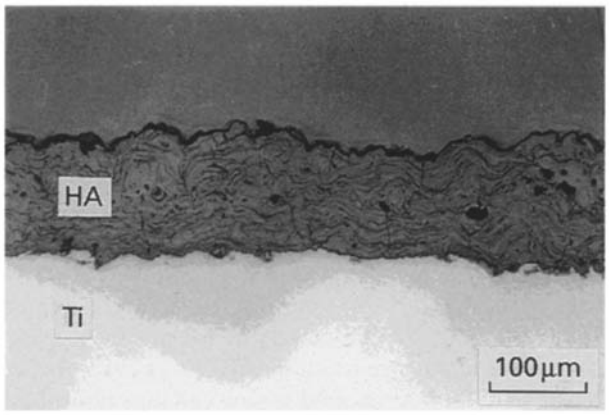

Figure 7 Optical micrograph of a transverse section through the HA coating (HA-hydroxyapatite, Ti-titanium alloy substrate).

The data obtained from both light microscopy and thermal wave interferometry are presented in Table II. The TWI measurements recorded at specific points along the scan line are given alongside the optical measurements taken from sections in the same regions, as indicated in Fig. 6. It can be seen that there is good agreement between microscopy measurements and the trace obtained using thermal wave interferometry, even in the critical region where the geometry of the prosthetic stem in changing. Furthermore, the relative magnitudes of the standard deviations are comparable for the two techniques. Fig. 7 shows a typical optical micrograph of a cross-section through a HA coating; the variability of the coating thickness can be seen to be approximately ± 15 μm.

4. Conclusions

The conventional method for analysing coatings involves producing sections which must be mounted and polished prior to using light microscopy and image analysis to establish accurate coating characteristics. The process is time consuming, expensive and destructive. By way of contrast, the thermal wave interferometry technique is rapid; the time taken to complete the 150 mm scan in this study was in the order of 10 minutes. It has the added advantage that it is non-destructive and non-contacting.

The present study established that good agreement could be found between the two sets of results obtained using conventional and TWI techniques. This indicates the enormous potential for the application of the latter technique to the accurate measurement of coating characteristics. The results confirm that thermal wave interferometry can cope with substantial variations in coating thickness on samples with a complex geometry.

A similar study was carried out on a total of seven different stem prostheses marketed by a number of different manufacturers. In each case very favourable agreements were obtained between TWI and optical microscopic measurements of coating thickness. This leads to the conclusion that TWI has the potential to provide a simple practical means of assessing HA coatings and of ensuring the quality and integrity of such coatings on prosthetic implants.

Acknowledgement

A. C. B. wishes to thank the Brazilian National Council CNPq-Brasilia/BRAZIL for personal financial support.

References

1. R. FIFIELD, *New Scientist* **116** (1987) 35.
2. D. F. WILLIAMS, *Met. & Mater.* **1** (1991) 24.
3. S. D. COOK, K. A. THOMAS, J. F. KAY and M. JARCHO, *Clin. Orthop. Rel. Res.* **230** (1988) 303.
4. A. DAVID, J. EITENMULLER, K. HANGST, H. F. BAR and G. MUHR, in Proceedings of Fourth World Biomaterials Congress, April 24–28 (1992) p. 98.
5. S. D. COOK, K. A. THOMAS, J. A. DALTON, T. S. WHITECLOUD and R. L. BARRACK, in Proceedings of the Fourth World Biomaterials Congress, April 24–28 (1992) p. 102.
6. P. DUCHEYNE, L. L. HENCH and A. KAGAN II, *J. Biomed. Mater. Res.* **14** (1988) 225.
7. K. DE GROOT, R. GEESINK and C. P. A. T. KLEIN, *ibid.* **21** (1987) 1375.
8. H. HERMAN, *Scientific American* **259** (1988) 78.
9. A. ROSENCWAIG and A. GERSHO, *J. Appl. Phys.* **47** (1976) 64.
10. H. VARGAS and L. C. M. MIRANDA, *Phys. Rep.* **161** (1988) 43.
11. C. A. BENNETT Jr. and R. R. PATTY, *Appl. Opt.* **21** (1982) 49.
12. P. M. PATEL, D. P. ALMOND and H. REITER, *Appl. Phys.* **B43** (1987) 9.
13. P. M. PATEL, D. P. ALMOND and J. D. MORRIS, *Eur. J. NDT.* **1** (1991) 64.

Received 7 July
and accepted 17 October 1994